Towards global weather forecasting with IFS-FVM

Christian Kühnlein, Peter Bechtold, Mauro Bianco[1], Willem Deconinck, Michail Diamantakis, Till Ehrengruber[1], Mike Gillard[2], Enrique González-Paredes[1], Rupert Klein[3], Linus Magnusson, Sylvie Malardel[4], Zbigniew Piotrowski[5], Piotr Smolarkiewicz[6], Tim Stockdale, Joanna Szmelter[2], Hannes Vogt[1], Nils Wedi

1) ETH Zurich/CSCS, Switzerland
2) University of Loughborough, UK
3) FU Berlin, Germany
4) Météo France, France
5) IMGW, Poland
6) NCAR, USA

$$\frac{\partial \mathcal{G}\rho}{\partial t} + \nabla \cdot (\mathbf{v}\mathcal{G}\rho) = 0$$

$$\frac{\partial \mathcal{G}\rho\mathbf{u}}{\partial t} + \nabla \cdot (\mathbf{v}\mathcal{G}\rho\mathbf{u}) = \mathcal{G}\rho\left(-\Theta_d\tilde{\mathbf{G}}\nabla\varphi' - \frac{\mathbf{g}}{\theta_a}\left(\theta' + \theta_a(\epsilon q_v' - q_c - q_r)\right) - \mathbf{f}\times\left(\mathbf{u} - \frac{\theta'}{\theta_a}\mathbf{u}_a\right) + \mathbf{M}(\mathbf{u}) + \mathbf{D}\right)$$

$$\frac{\partial \mathcal{G}\rho\theta'}{\partial t} + \nabla \cdot (\mathbf{v}\mathcal{G}\rho\theta') = \mathcal{G}\rho\left(-\tilde{\mathbf{G}}^T\mathbf{u}\cdot\nabla\theta_a - \frac{L}{c_p\pi}\left(\frac{\Delta q_{vs}}{\Delta t} + E_r\right) + \mathcal{H}\right)$$

$$\frac{\partial \mathcal{G}\rho q_k}{\partial t} + \nabla \cdot (\mathbf{v}\mathcal{G}\rho q_k) = \mathcal{G}\rho\mathcal{R}^{q_k}$$

$$\frac{\partial \mathcal{G}\rho\varphi'}{\partial t} + \nabla \cdot (\mathbf{v}\mathcal{G}\rho\varphi') = \mathcal{G}\rho\sum_{\ell=1}^{3}\left(\frac{a_\ell}{\zeta_\ell}\nabla\cdot\zeta_\ell(\check{\mathbf{v}} - \tilde{\mathbf{G}}^T\mathbf{C}\nabla\varphi')\right) + b\varphi' + c$$

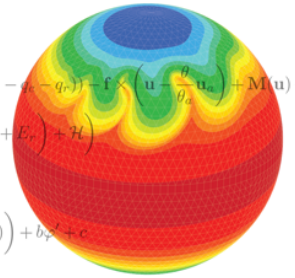

© ECMWF September 15, 2020

IFS dynamical core options at ECMWF

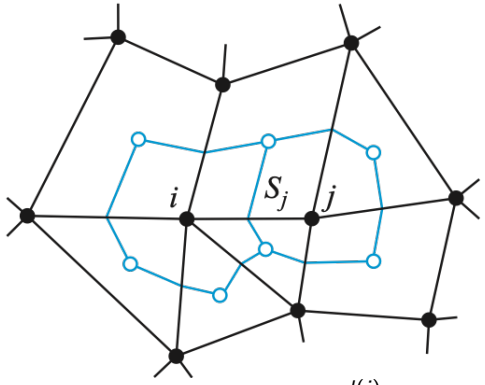

$$\int_\Omega \nabla\cdot\mathbf{A} = \int_{\partial\Omega} \mathbf{A}\cdot\mathbf{n} = \frac{1}{\mathcal{V}_i}\sum_{j=1}^{I(i)} A_j^{\perp} S_j$$

dual volume: $\mathcal{V}_i$, face area: S_j

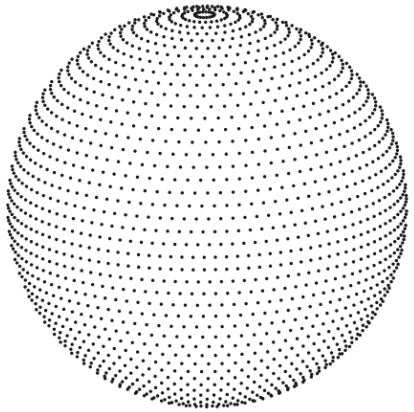

O24 grid points

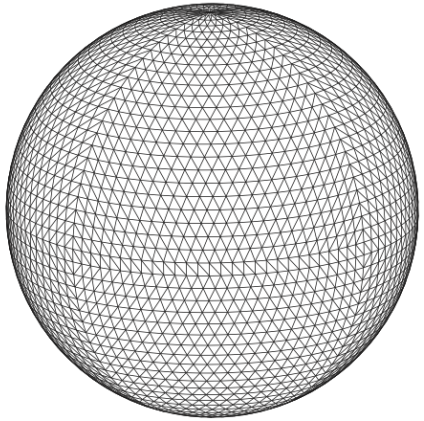

Primary mesh O24

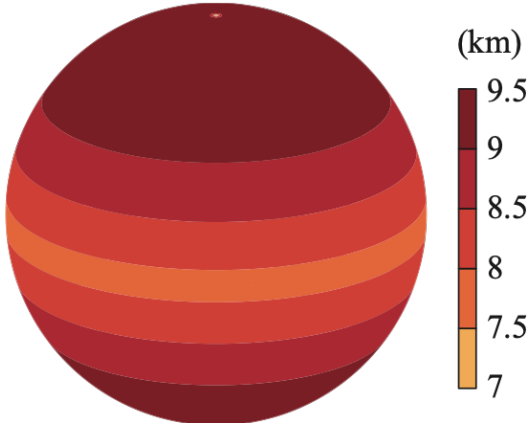

O1280 dual mesh spacing

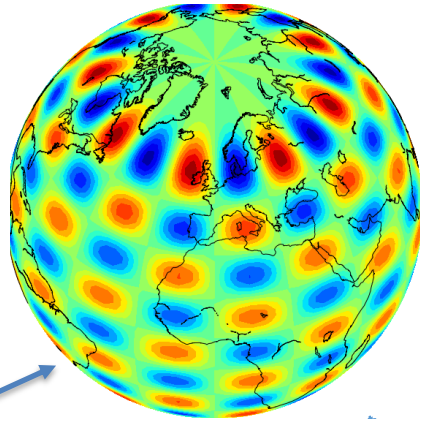

| currently operational |

Model aspect	IFS-FVM	IFS-ST	IFS-ST (NH option)
Equation system	fully compressible	hydrostatic primitive	fully compressible
Prognostic variables	$\rho_d, u, v, w, \theta', \varphi', r_v, r_l, r_r, r_i, r_s$	$\ln p_s, u, v, T_v, q_v, q_l, q_r, q_i, q_s$	$\ln \pi_s, u, v, d_4, T_v, \hat{q}, q_v, q_l, q_r, q_i, q_s$
Horizontal coordinates	λ, ϕ (lon–lat)	λ, ϕ (lon–lat)	λ, ϕ (lon–lat)
Vertical coordinate	generalized height	hybrid sigma–pressure	hybrid sigma–pressure
Horizontal discretization	unstructured finite volume (FV)	spectral transform (ST)	spectral transform (ST)
Vertical discretization	structured FD–FV	structured FE	structured FD or FE
Horizontal staggering	co-located	co-located	co-located
Vertical staggering	co-located	co-located	co-located, Lorenz
Horizontal grid	octahedral Gaussian or arbitrary	octahedral Gaussian	octahedral Gaussian
Time stepping scheme	2-TL SI	2-TL constant-coefficient SI	2-TL constant-coefficient SI with ICI
Advection	conservative FV Eulerian	non-conservative SL	non-conservative SL

IFS-FVM fully compressible equations

$$\frac{\partial \mathscr{G}\rho_d}{\partial t} + \nabla\cdot(\mathbf{v}\mathscr{G}\rho_d) = 0\,,$$

$$\frac{\partial \mathscr{G}\rho_d\mathbf{u}}{\partial t} + \nabla\cdot(\mathbf{v}\mathscr{G}\rho_d\mathbf{u}) = \mathscr{G}\rho_d\left[-\theta_\rho\widetilde{\mathbf{G}}\nabla\varphi' - \theta_\rho\widetilde{\mathbf{G}}\nabla\varphi_a + \mathbf{g} - \mathbf{f}\times\mathbf{u} + \mathbf{M}(\mathbf{u}) + \boldsymbol{P}^{\mathbf{u}}\right]\,,$$

$$\frac{\partial \mathscr{G}\rho_d\theta'}{\partial t} + \nabla\cdot\left(\mathbf{v}\mathscr{G}\rho_d\,\theta'\right) = \mathscr{G}\rho_d\left[-\widetilde{\mathbf{G}}^T\mathbf{u}\cdot\nabla\theta_a + P^\theta\right]\,,$$

$$\frac{\partial \mathscr{G}\rho_d\,r_k}{\partial t} + \nabla\cdot(\mathbf{v}\mathscr{G}\rho_d\,r_k) = \mathscr{G}\rho_d P^{r_k}\,, \qquad r_k = r_v\,, r_l\,, r_r\,, r_i\,, r_s$$

$$\frac{\partial \mathscr{G}\rho_d\,\Lambda_a}{\partial t} + \nabla\cdot(\mathbf{v}\mathscr{G}\rho_d\,\Lambda_a) = \mathscr{G}\rho_d P^{\Lambda_a}\,,$$

$$\varphi' = c_{pd}\left[\left(\frac{R_d}{p_0}\rho_d\,\theta\,(1 + r_v/\varepsilon)\right)^{R_d/c_{vd}} - \pi_a\right]\,.$$

Building on:
Kühnlein et al. GMD 2019
Smolarkiewicz et al. JCP 2019

$$\theta_\rho = \frac{1 + r_v/\varepsilon}{1 + r_t}\theta\,, \qquad r_t = \sum r_k = r_v + r_l + r_r + r_s + r_i \qquad \varphi' = \varphi - \varphi_a\,, \qquad \theta' = \theta - \theta_a$$

IFS-FVM two-time-level semi-implicit integration

$$\frac{\partial G\Psi}{\partial t} + \nabla \cdot (\boldsymbol{V}\Psi) = G\left(\mathcal{R}^{\Psi} + P^{\Psi}\right) ,$$

$$\Psi_{\boldsymbol{i}}^{n+1} = \mathcal{A}_{\boldsymbol{i}}(\widetilde{\Psi}, \boldsymbol{V}^{n+1/2}, G^{n}, G^{n+1}, \delta t) + b^{\Psi}\,\delta t\,\mathcal{R}^{\Psi}|_{\boldsymbol{i}}^{n+1}$$
$$\equiv \widehat{\Psi}_{\boldsymbol{i}} + b^{\Psi}\,\delta t\,\mathcal{R}^{\Psi}|_{\boldsymbol{i}}^{n+1} ,$$

$$\widetilde{\Psi} = \Psi^{n} + a^{\Psi}\,\delta t\,\mathcal{R}^{\Psi}|^{n} + \delta t\,P^{\Psi}|^{n} ,$$

Variable	Ψ	$\boldsymbol{V}$	G	a^{Ψ}	b^{Ψ}
Dry density	ρ_{d}	$\boldsymbol{v}\mathcal{G}$	$\mathcal{G}$	–	–
Zonal physical velocity	u	$\boldsymbol{v}\mathcal{G}\rho_{\mathrm{d}}$	$\mathcal{G}\rho_{\mathrm{d}}$	0.5	0.5
Meridional physical velocity	v	$\boldsymbol{v}\mathcal{G}\rho_{\mathrm{d}}$	$\mathcal{G}\rho_{\mathrm{d}}$	0.5	0.5
Vertical physical velocity	w	$\boldsymbol{v}\mathcal{G}\rho_{\mathrm{d}}$	$\mathcal{G}\rho_{\mathrm{d}}$	0.5	0.5
Potential temperature perturbation	θ'	$\boldsymbol{v}\mathcal{G}\rho_{\mathrm{d}}$	$\mathcal{G}\rho_{\mathrm{d}}$	0.5	0.5
Water vapour mixing ratio	r_{v}	$\boldsymbol{v}\mathcal{G}\rho_{\mathrm{d}}$	$\mathcal{G}\rho_{\mathrm{d}}$	–	–
Liquid water mixing ratio	r_{l}	$\boldsymbol{v}\mathcal{G}\rho_{\mathrm{d}}$	$\mathcal{G}\rho_{\mathrm{d}}$	–	–
Rain water mixing ratio	r_{r}	$\boldsymbol{v}\mathcal{G}\rho_{\mathrm{d}}$	$\mathcal{G}\rho_{\mathrm{d}}$	–	–
Ice mixing ratio	r_{i}	$\boldsymbol{v}\mathcal{G}\rho_{\mathrm{d}}$	$\mathcal{G}\rho_{\mathrm{d}}$	–	–
Snow mixing ratio	r_{s}	$\boldsymbol{v}\mathcal{G}\rho_{\mathrm{d}}$	$\mathcal{G}\rho_{\mathrm{d}}$	–	–
Cloud fraction	Λ_{a}	$\boldsymbol{v}\mathcal{G}\rho_{\mathrm{d}}$	$\mathcal{G}\rho_{\mathrm{d}}$	–	–
Exner pressure perturbation	φ'	$\boldsymbol{v}\mathcal{G}\rho_{\mathrm{d}}$	$\mathcal{G}\rho_{\mathrm{d}}$	$(1-\alpha)$	α

- NFT-MPDATA approach (Smolarkiewicz and Grabowski JCP 1990, Smolarkiewicz and Margolin JCP 1998, Smolarkiewicz and Szmelter JCP 2005, Kühnlein and Smolarkiewicz JCP 2017, Kühnlein et al. GMD 2019)
- 3D implicit treatment of fast (acoustic, buoyant) and slow terms
- Implicit acoustic scheme results in 3D Helmholtz problem for Exner pressure perturbation solved by a preconditioned Krylov approach (Smolarkiewicz and Szmelter AG 2011, Smolarkiewicz et al. JCP 2014, Smolarkiewicz et al. JCP 2016, Kühnlein et al. GMD 2019)

IFS-FVM comparison with IFS-ST: baroclinic instability benchmark test

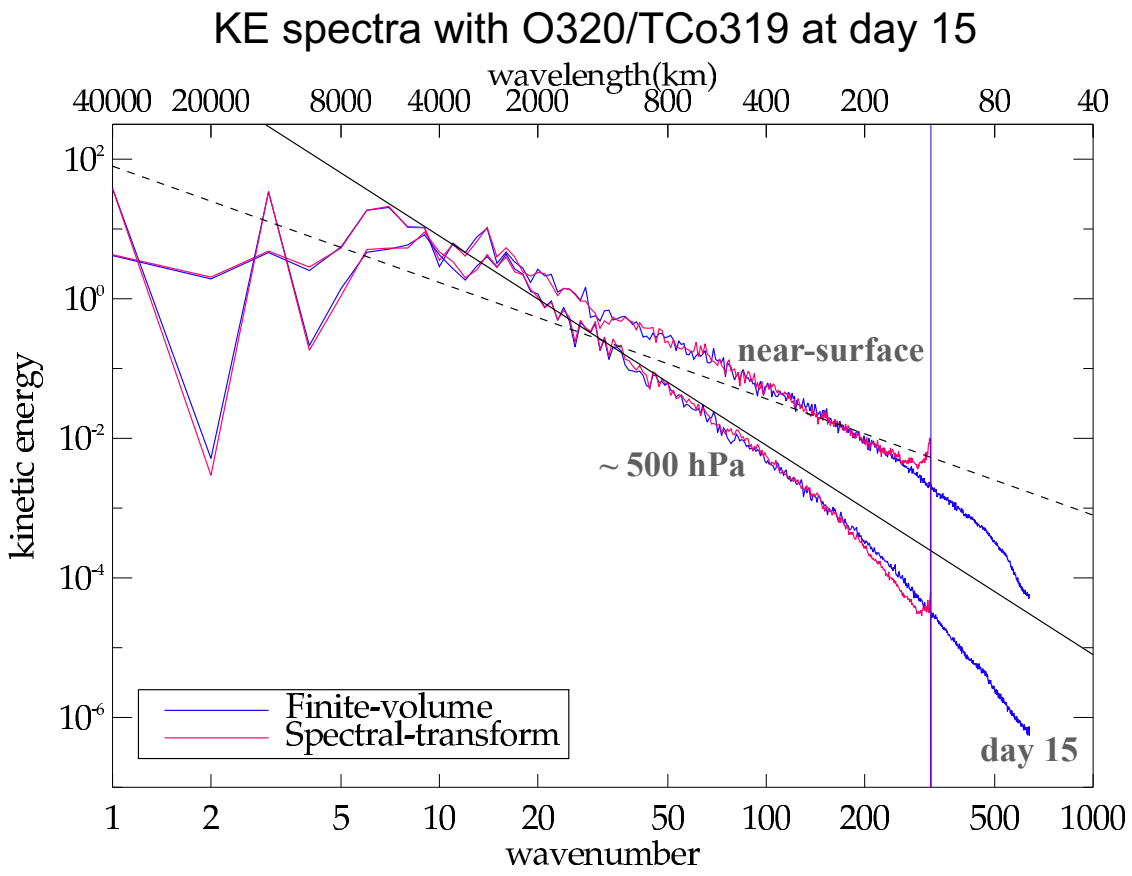

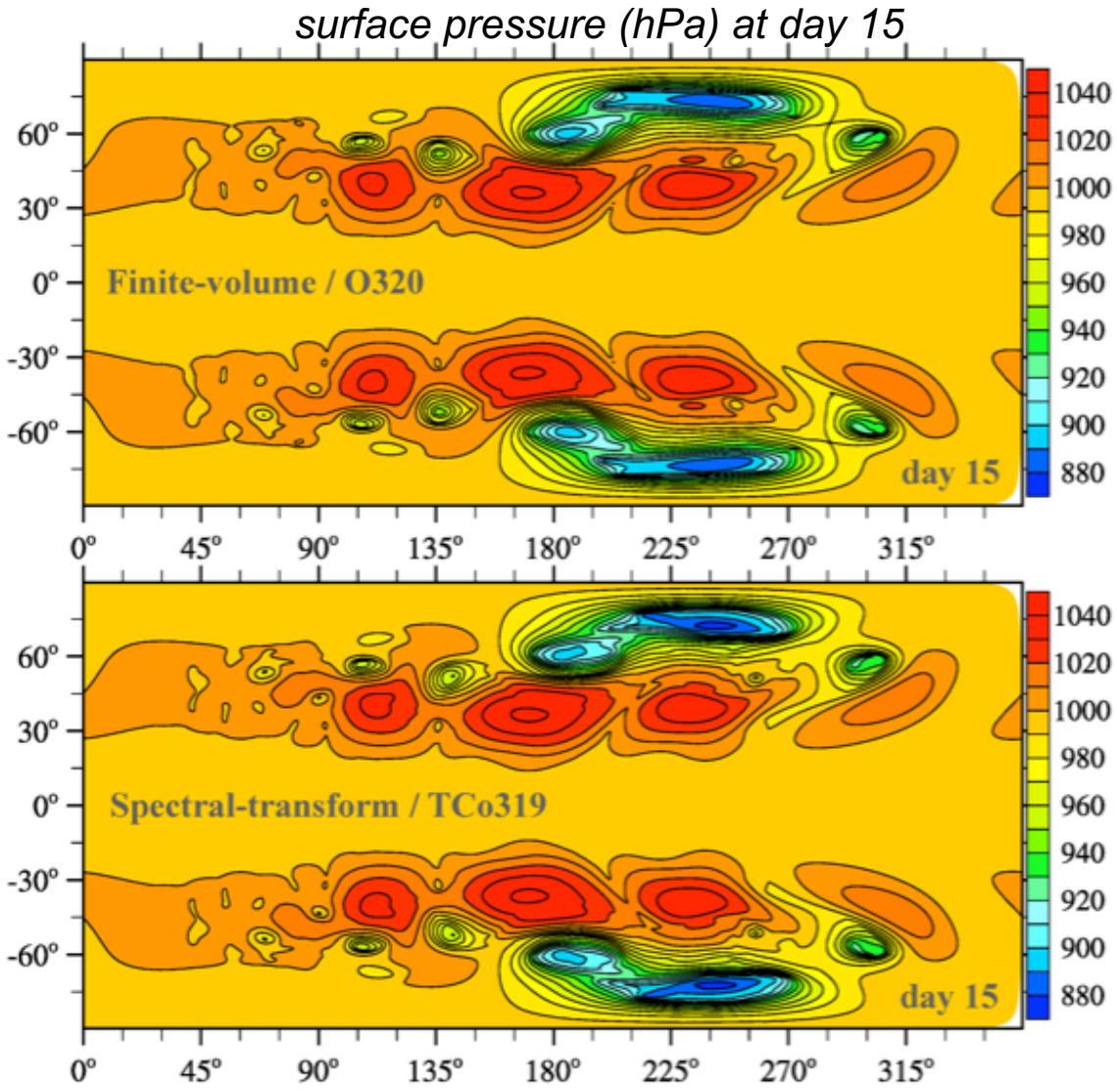

Kühnlein et al. GMD 2019 32km

Computational efficiency for baroclinic instability

- Baroclinic instability experiments in identical configuration O1280/TCo1279 (9km) with L137
- IFS-ST CY43R3, dt=450s, DP
- IFS-FVM, avg. dt=80s, DP
- timings obtained as average over days 10-15 of simulation
- no physics!

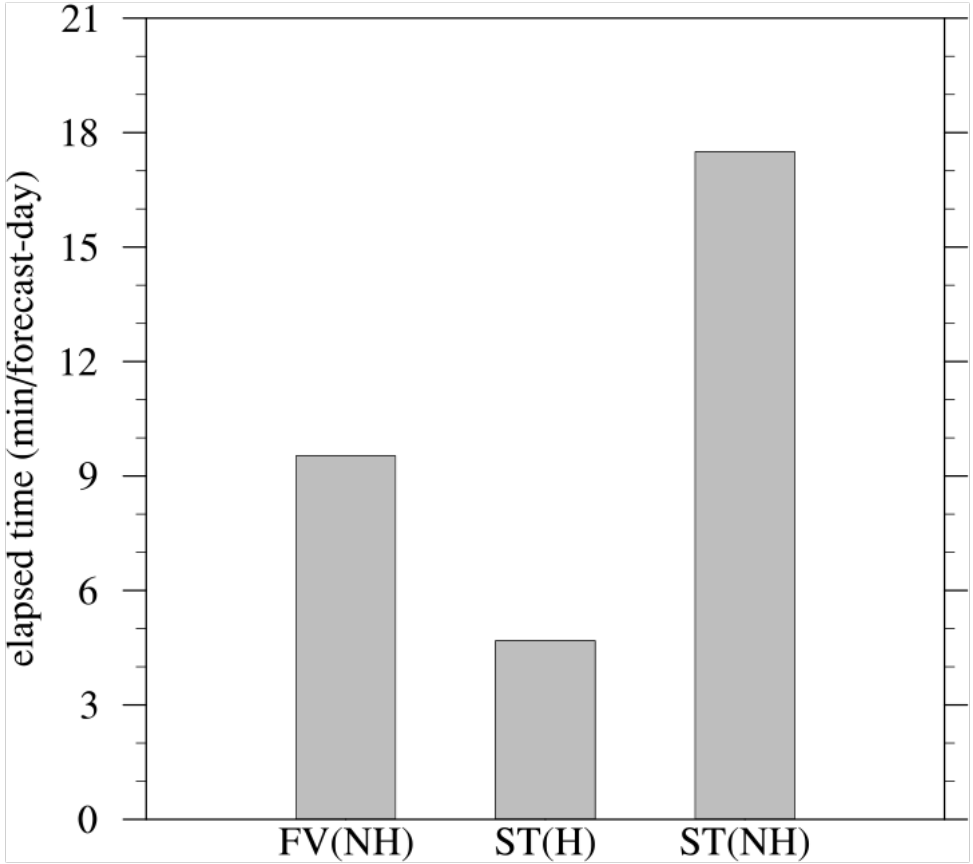

O1280/TCo1279 with L137 dycore on 350 nodes of ECMWF's Cray XC40

Kühnlein et al. GMD 2019

Stratified flow past Schär (circular) mountain in small-planet configuration

MPAS

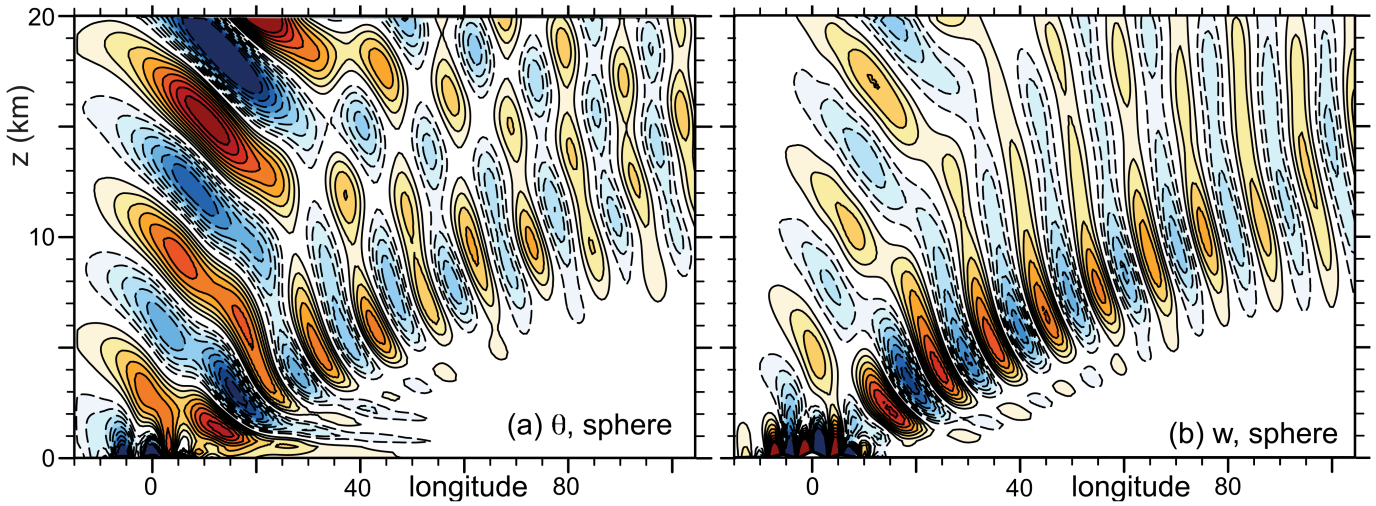

MPAS results from
Klemp et al. JAMES 2015

solutions after 2h

IFS-FVM

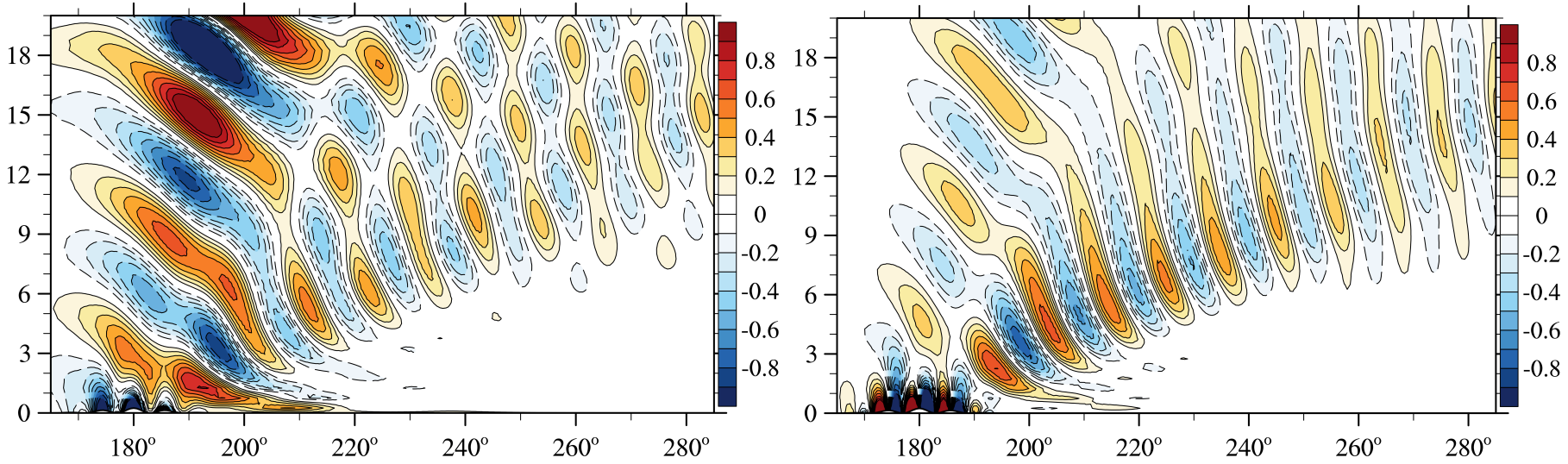

→ see also Zarzycki et al. GMD 2019 for DCMIP16 splitting supercell model comparison

IFS-FVM coupling to IFS physical parametrisations

- stand-alone implementation of FVM with IFS physical parametrisation package CY43R3
- Bespoke FVM interface
- ecRad radiation scheme on model grid (called 1h-3h)
- As the current default, tendencies from IFS physical parametrizations are incorporated in FVM SI scheme using Euler forward approach with subcycling of dynamics:

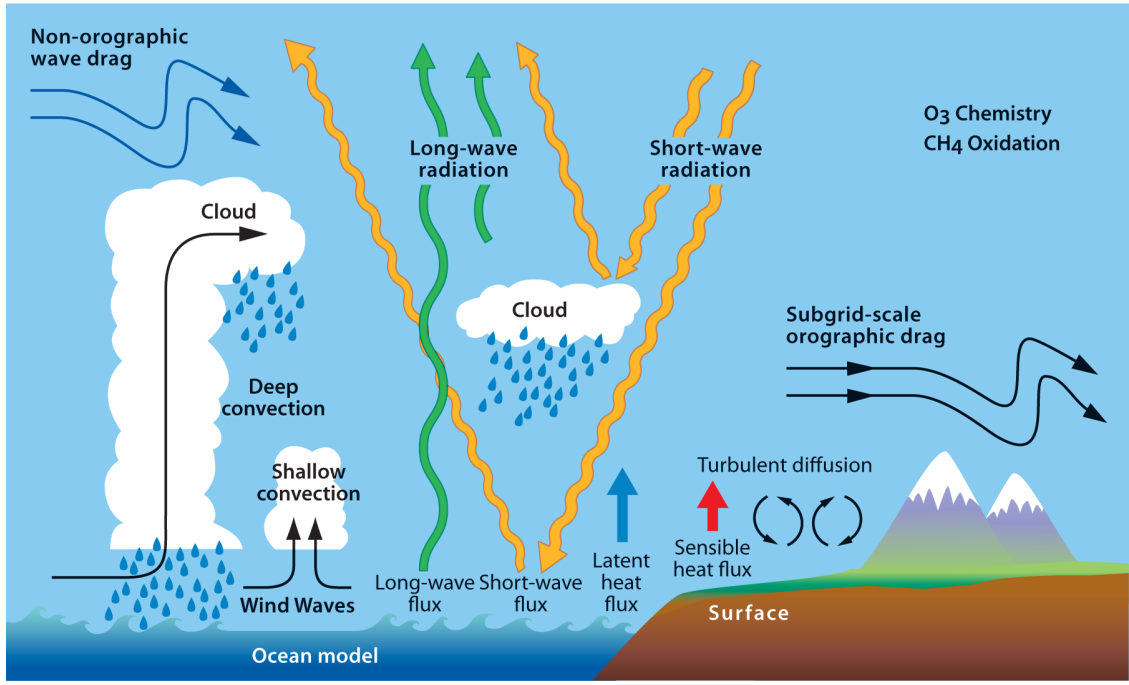

Physics time step from t^N to $t^N + \Delta t_{phys} \equiv t^N + N_s\,\delta t$ for $\ell = 1, N_s$:

$$\Psi_{\mathbf{i}}\left(t^N + \ell\delta t\right) = \mathscr{A}_{\mathbf{i}}\left(\widetilde{\Psi}, \mathbf{V}(t^N + (\ell\delta t - 0.5)), G(t^N + (\ell-1)\delta t), G(t^N + \ell\delta t), \delta t\right) + b^{\Psi}\,\delta t\,\mathscr{R}_{\mathbf{i}}^{\Psi}\left(t^N + \ell\delta t\right)$$

$$\widetilde{\Psi} = \Psi\left(t^N + (\ell-1)\delta t\right) + a^{\Psi}\,\delta t\,\mathscr{R}^{\Psi}\left(t^N + (\ell-1)\delta t\right) + \delta t\,P^{\Psi}\left(t^N, \Delta t_{phys}\right)$$

IFS-FVM real weather configuration

- Initialisation procedures for FVM prognostic variables from IFS analysis
- Procedures to generate and initialise FVM ambient states using analytical functions or reanalysis data
- Surface fields identical to IFS, including resolved orography

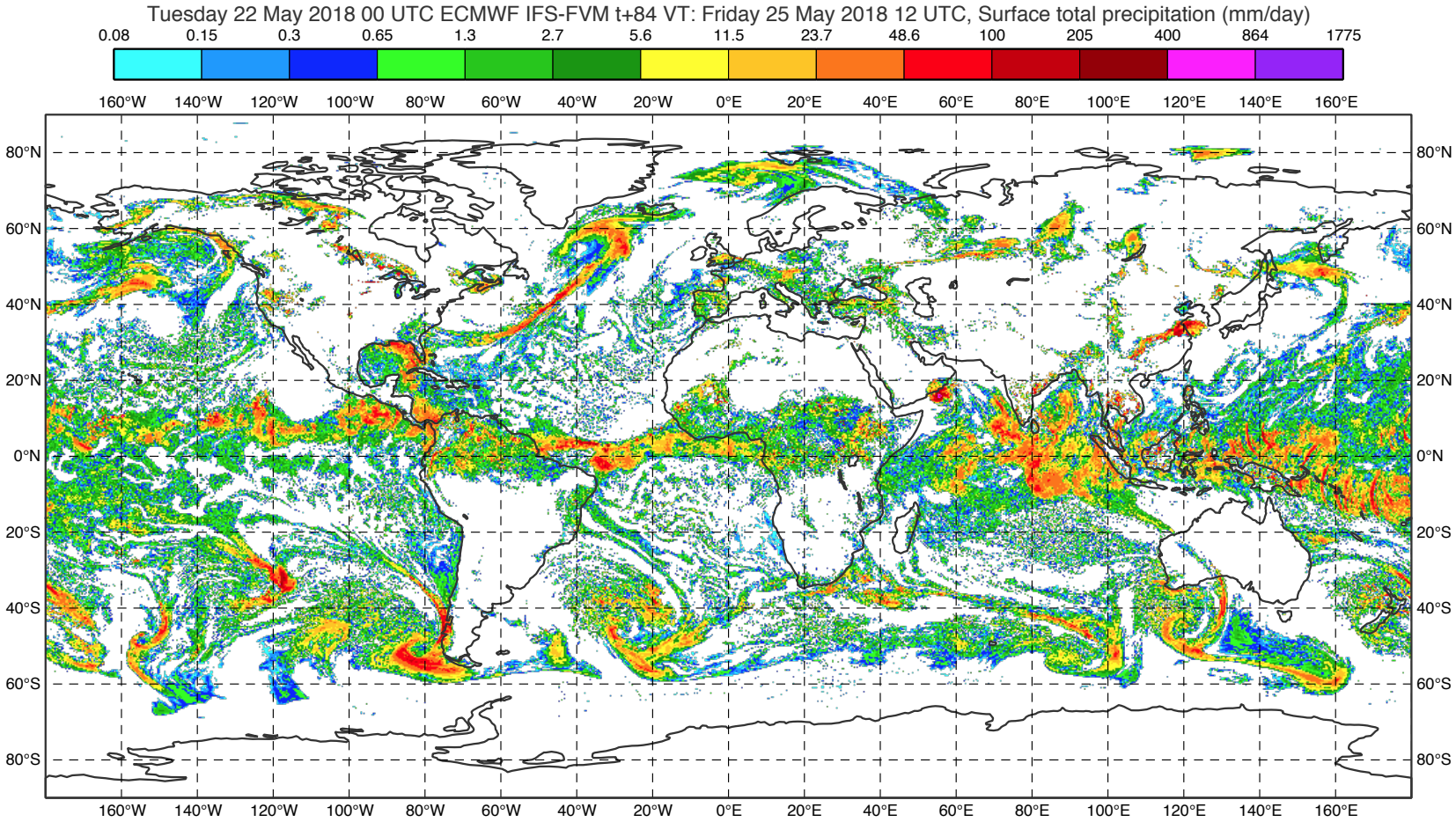

- Initialisation from IFS analysis 20180522 00 UTC
- O1280 corresponding to ~9 km nominal spacing, L62
- IFS physics CY43R3, ecRad on O1280 grid, uncoupled

ECMWF

IFS-FVM ongoing case study of Hurricane IRMA

- Major Hurricane of Category 5 in tropical Atlantic

- Formed 30 August 2017
- Dissipated 14 September 2017

- 285 km/h 1-minute sustained winds

- 914 hPa minimum MSLP

- Peak intensity on 5 September 2017

- Fourth-costliest tropical cyclone on record

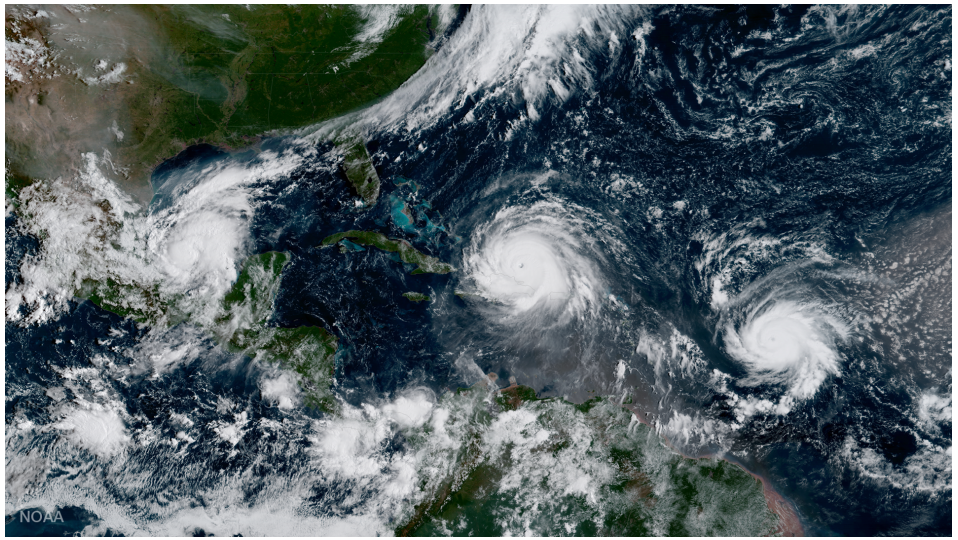

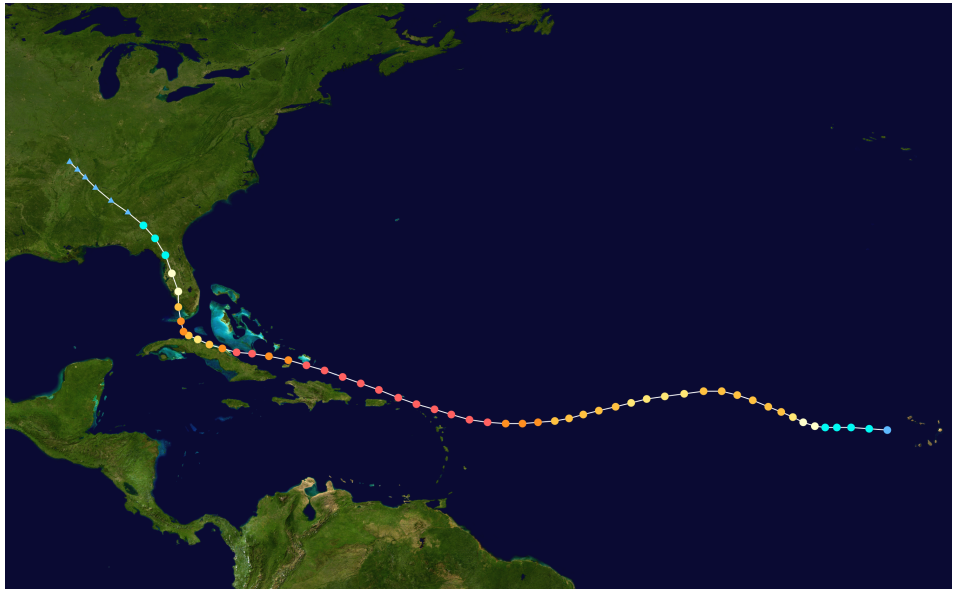

ECMWF

IFS-FVM forecast experiments of Hurricane IRMA

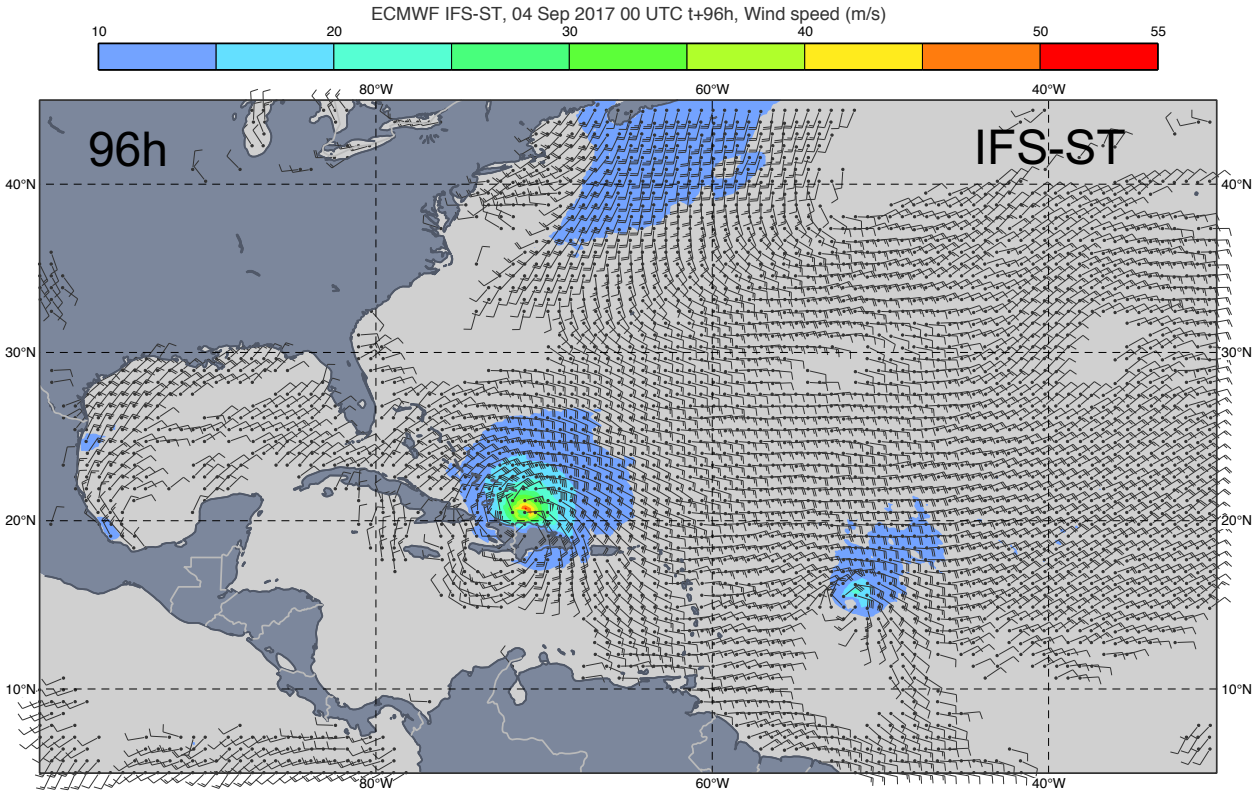

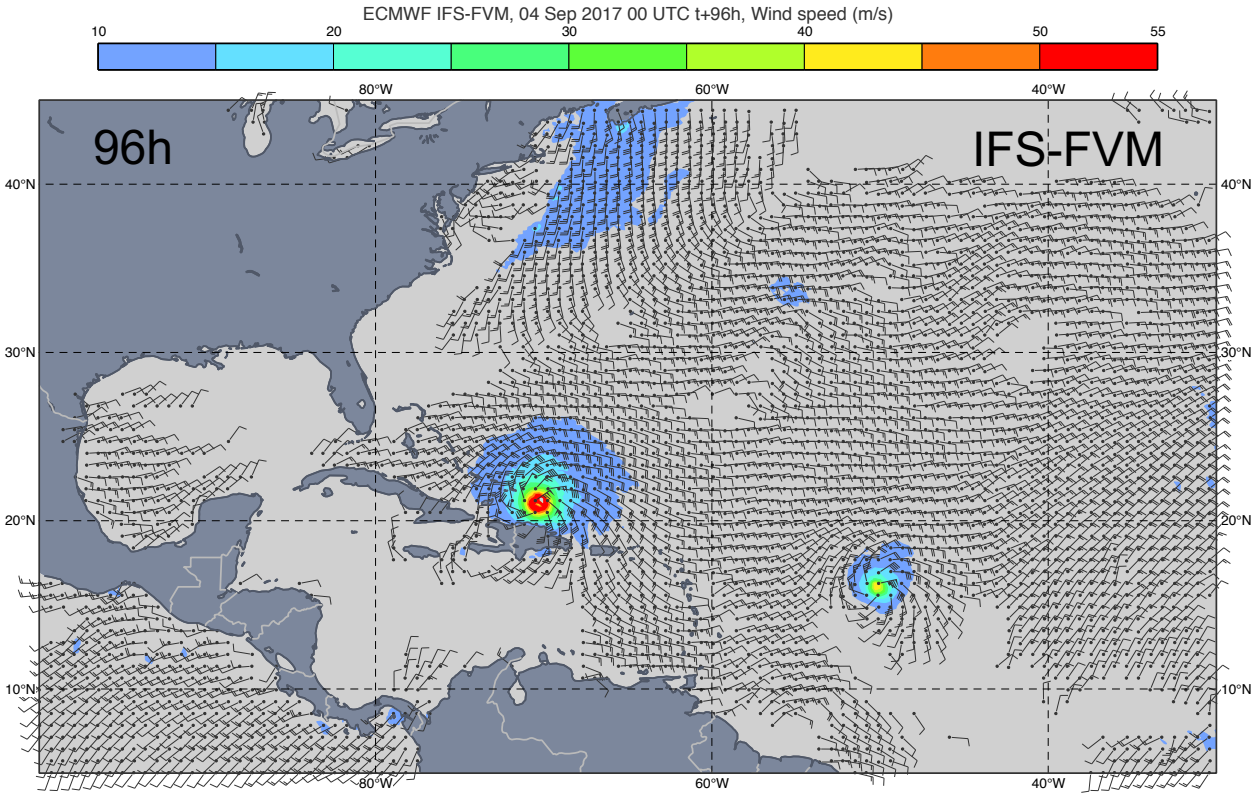

- Initialisation from IFS analysis 20170904 00 UTC
- O1280/TCo1279 corresponding to ~9 km nominal spacing, L62
- IFS CY43R3, uncoupled

ECMWF

IFS-FVM forecast experiments of Hurricane IRMA

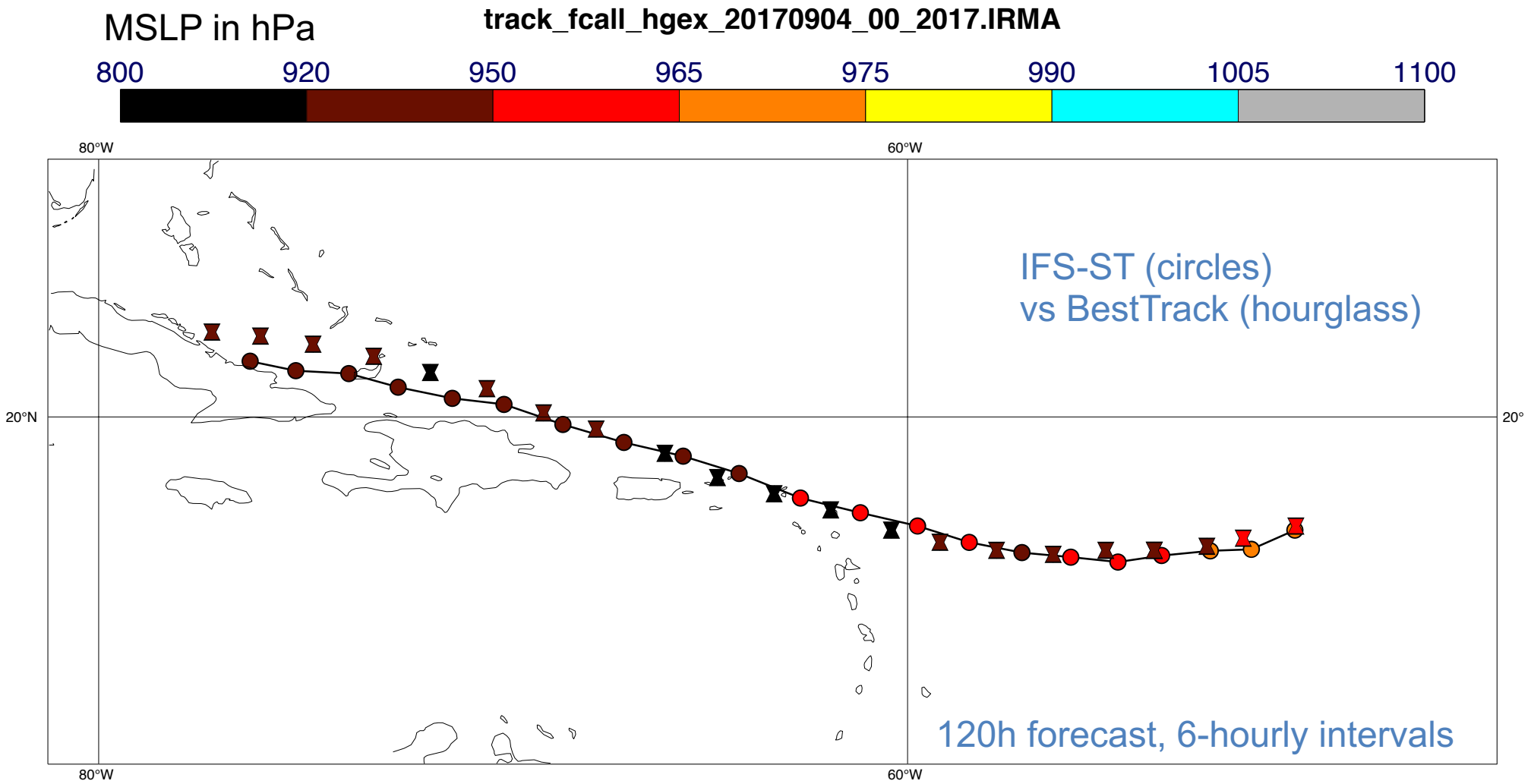

- Initialisation from IFS analysis 20170904 00 UTC
- O1280/TCo1279 corresponding to ~9 km nominal spacing, L62
- IFS CY43R3, uncoupled

ECMWF

IFS-FVM forecast experiments of Hurricane IRMA

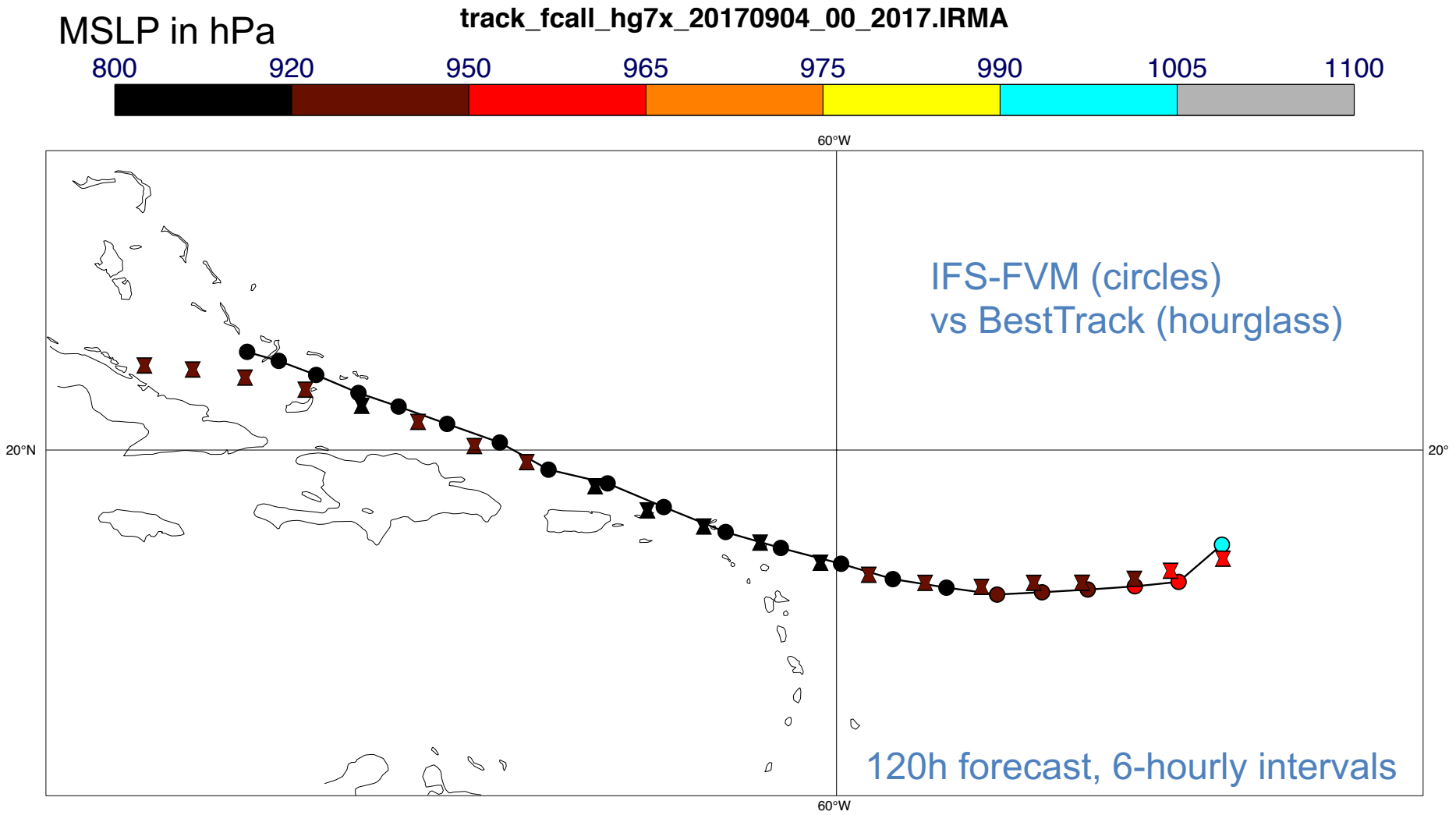

- Initialisation from IFS analysis 20170904 00 UTC
- O1280/TCo1279 corresponding to ~9 km nominal spacing, L62
- IFS CY43R3, uncoupled

ECMWF

IFS-FVM forecast experiments of Hurricane IRMA

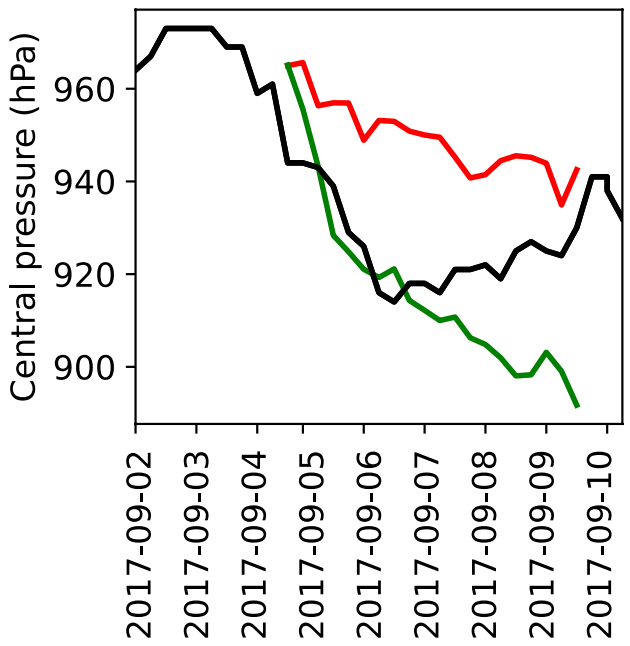

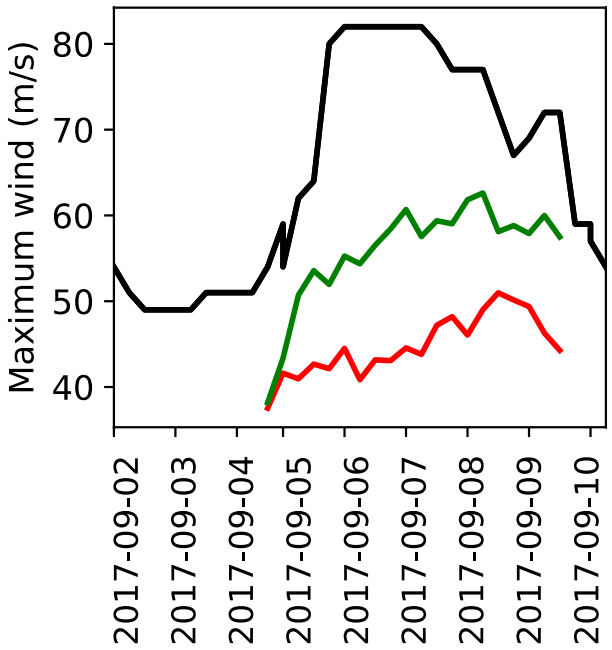

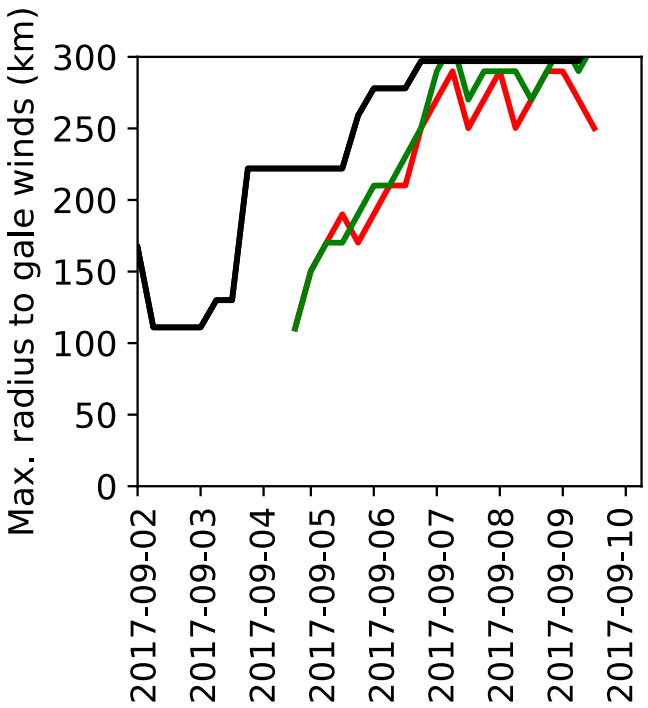

IFS-ST
IFS-FVM
BestTrack

32-bit precision implementation of IFS-FVM

MPI x OMP	72 x 18	144 x 9	144 x 18	288 x 9
SP	2315 s	2365 s	1260 s	1269 s
DP	3660 s	3634 s	2007 s	1926 s

- Runtimes for a O640/L62 4-day forecast using single- vs. double-precision on Cray XC40
- Configuration is for init date 22 May 2018 00 UTC, full IFS physics package, all parametrisations apart from radiation and non-orographic GW drag are called at every FVM time step here (usually run with subcycling for efficiency)
- Radiation called every hour and run on same O640 grid
- Convergence of the FVM preconditioned Krylov solver is essentially identical with SP and DP given typical thresholds

IFS-FVM implementation in the GT4Py DSL of ETHZ+CSCS

- Starting point is FVM in modern Fortran with MPI/OpenMP parallelisation targeting CPUs and using the Atlas framework
- Separation of concerns in model implementation with Domain-Specific Language
- Sustainable coding implementation wrt future HPC
- GT4Py DSL developed to support all requirements of the IFS-FVM discretisation
- Rewrite IFS-FVM in GT4Py DSL and the GridTools framework developed at ETH Zurich and the Swiss National Supercomputing Centre CSCS
- Started collaboration in 2020

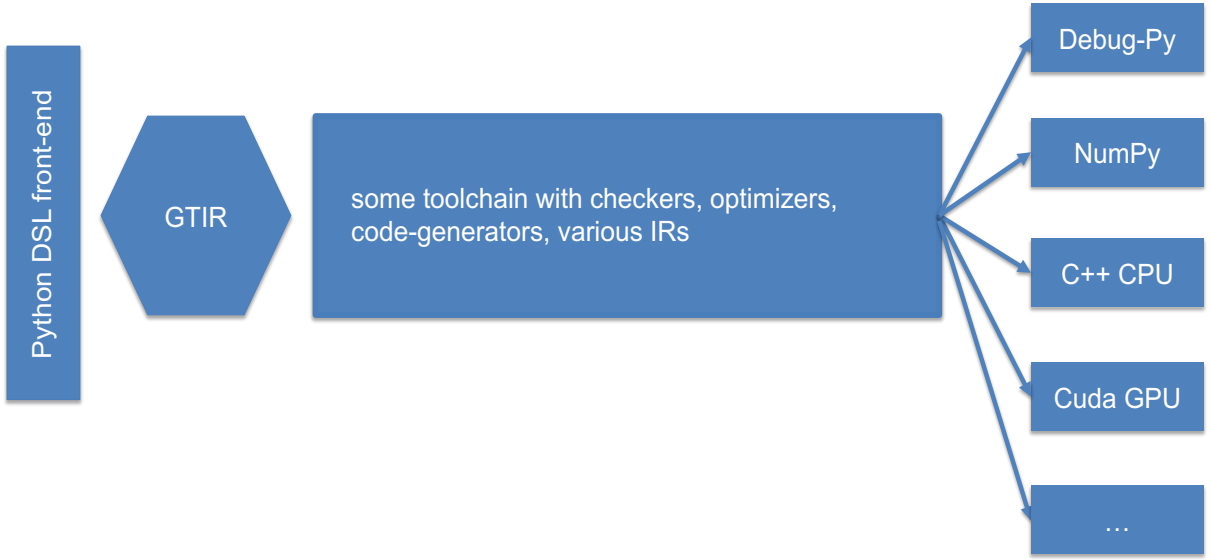


```
@gtscript.stencil
def div_stencil(
        mesh:   Mesh,                                   # computational domain
        S:      Field[Edge, Vec[float, 2]]              # oriented surface
        rho:    Field[Vertex, float]                    # density
        vel:    Field[Vertex, Vec[float, 2]],           # velocity
        div:    Field[Vertex, float],                   # discrete divergence operator
        sign:   Field[[Vertex, Local[Edge]], float]     # face orientation
):
    with computation(PARALLEL): # iteration order of the vertical axes
        with edges(mesh) as e: # computation on edges
            flux_density = 0.5*sum(rho[v] * vel[v] for v in vertices(e)) # flux density on face
            flux = dot(S, flux_density)                                  # flux on a face
        with vertices(mesh) as v: # computation on vertices
            div = sum(flux[e] * sign[v, e] for e in edges(v))
```

IFS-FVM ongoing and future work

- Refine and extend FVM and its coupling to IFS physical parametrisations for ECMWF forecast configurations
- DSL implementation based on GT4Py and the GridTools framework in scollaboration with ETHZ+CSCS
- Development and evaluation of FVM, also for LAM applications, e.g. at Météo France and in the Aladin Consortium
- FV/SL/SL-DG multi-tracer advective transport (Michail Diamantakis, Giovanni Tumolo)
- Tangent-linear and adjoint of IFS-FVM needed for 4DVAR data assimilation (Filip Vana)
- Earth-System configuration with coupled ocean, sea-ice and wave model

Finite-Volume Module of the IFS

IFS-FVM dynamical core option:

- nonhydrostatic, deep-atmosphere, fully compressible equations in perturbation form
- horizontally-unstructured vertically-structured median-dual finite-volume discretisation
- nonoscillatory flux-form multidimensional and HV-split Eulerian advection
- spatio-temporal semi-implicit integration congruent with semi-Lagrangian approach
- octahedral grid, co-located prognostic variables with IFS-ST
- Atlas mesh and parallel datastructures
- Fortran code and using hybrid MPI/OpenMP for CPUs
- 64-bit or 32-bit precision
- stand-alone IFS-FVM coupled to IFS physical parametrisation package (CY43R3)
- ecRad radiation scheme on model grid

Smolarkiewicz et al. JCP 2016
Kühnlein et al. GMD 2019

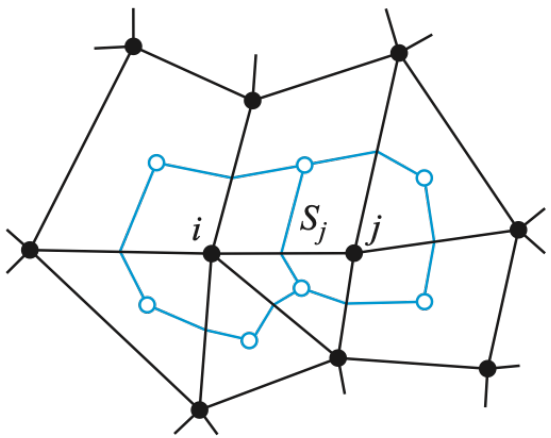

$$\int_\Omega \nabla\cdot\mathbf{A} = \int_{\partial\Omega} \mathbf{A}\cdot\mathbf{n} = \frac{1}{\mathcal{V}_i}\sum_{j=1}^{l(i)} A_j^{\perp} S_j$$

dual volume: $\mathcal{V}_i$, face area: S_j

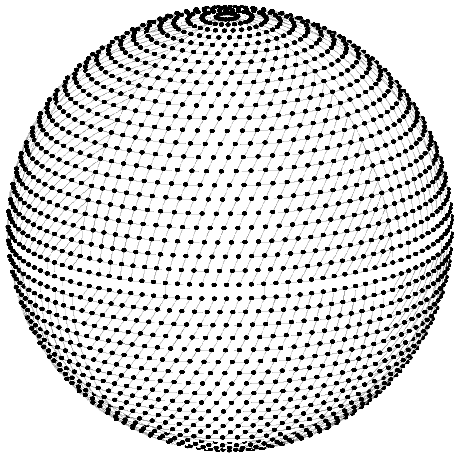

Nodes of octahedral grid O24

DCMIP2016 dynamical core intercomparison: splitting supercell

vertical velocity (m/s) in lon-lat section at z=5km

rain water (g/kg) in lon-lat section at z=5km

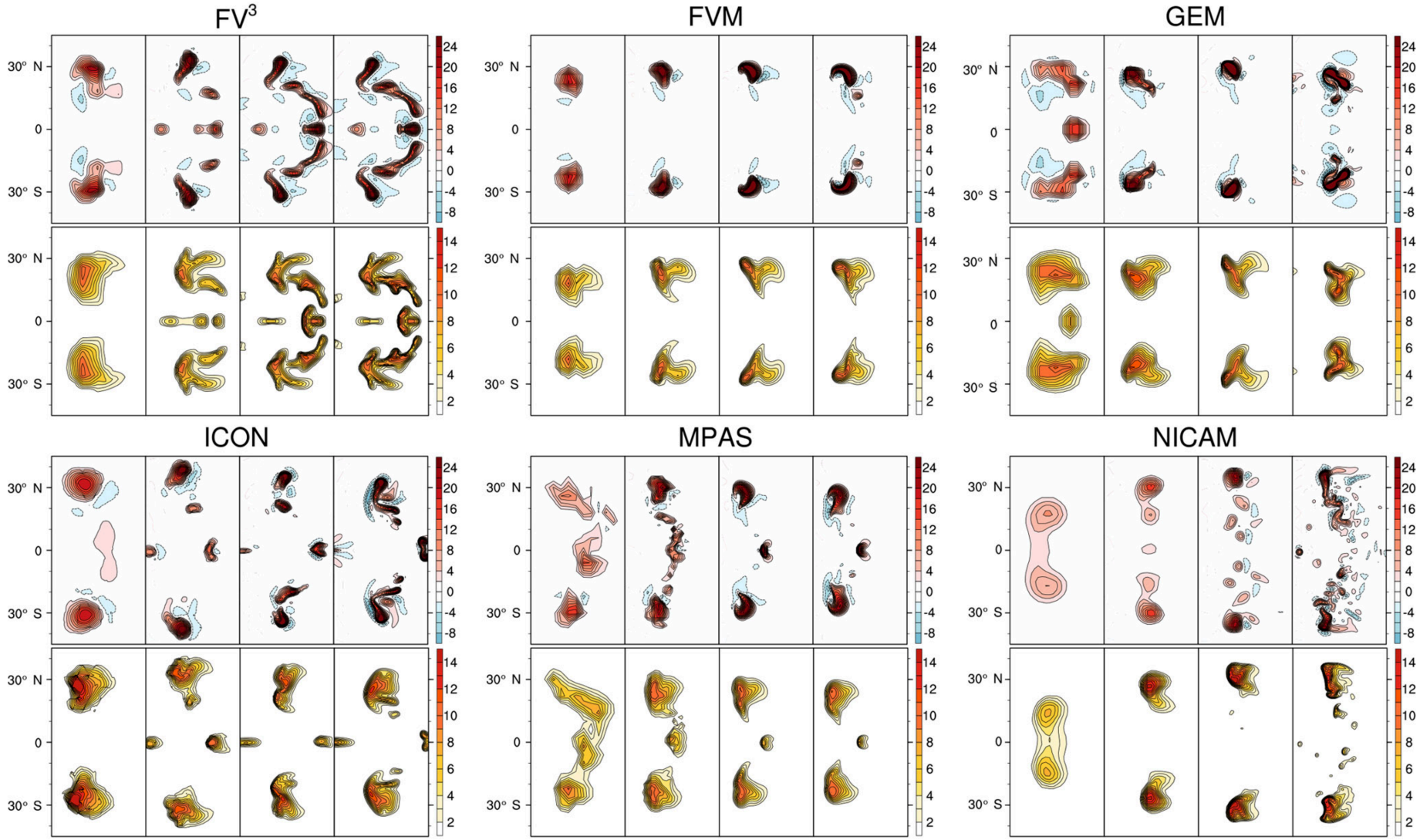

final 2h result as various grid spacing (panels are at 4, 2, 1, 0.5 km)

Zarzycki et al. GMD 2019

DCMIP2016 dynamical core intercomparison: splitting supercell

Zarzycki et al. GMD 2019

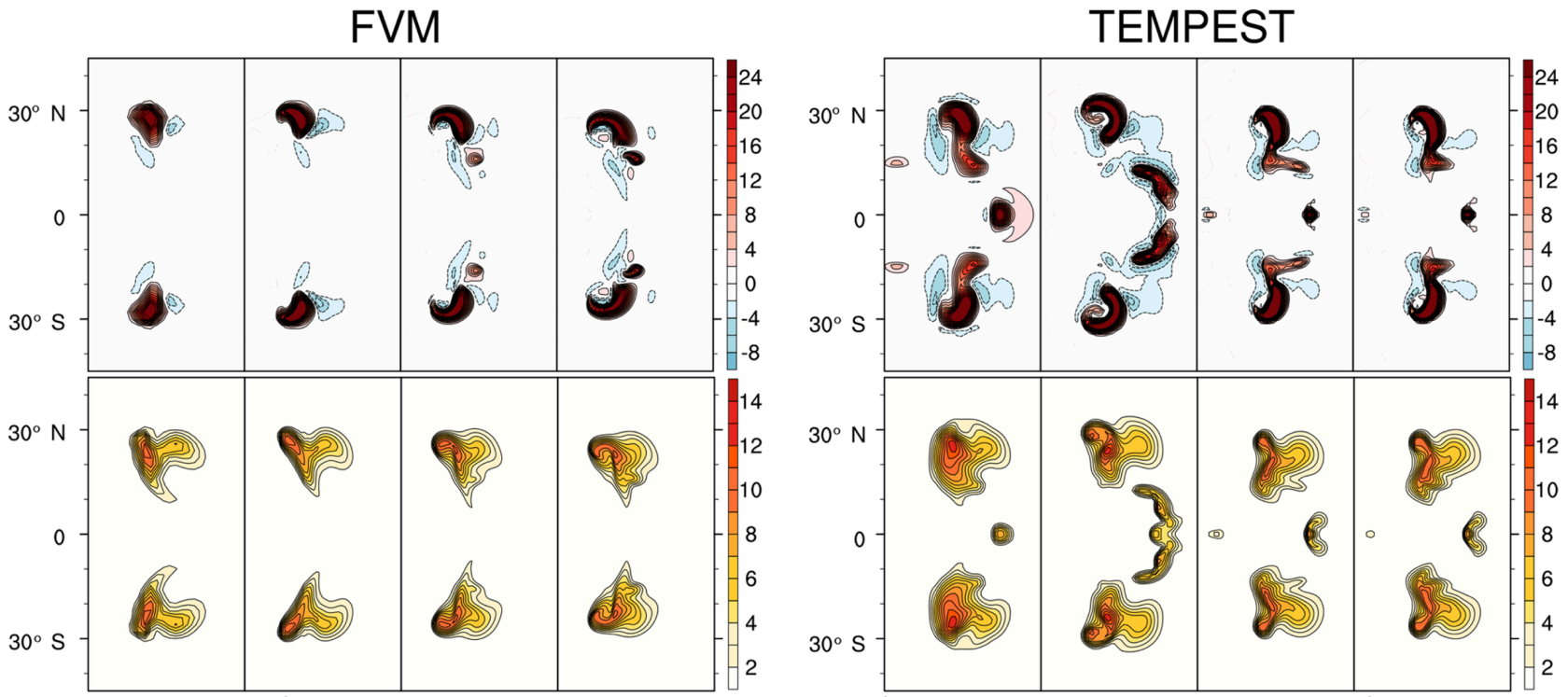

final 2h result as various grid spacings (panels are at 2, 1, 0.5, 0.25 km)

→ FVM uses second-order Finite-Volume method

→ TEMPEST uses higher-order Spectral-Element methods
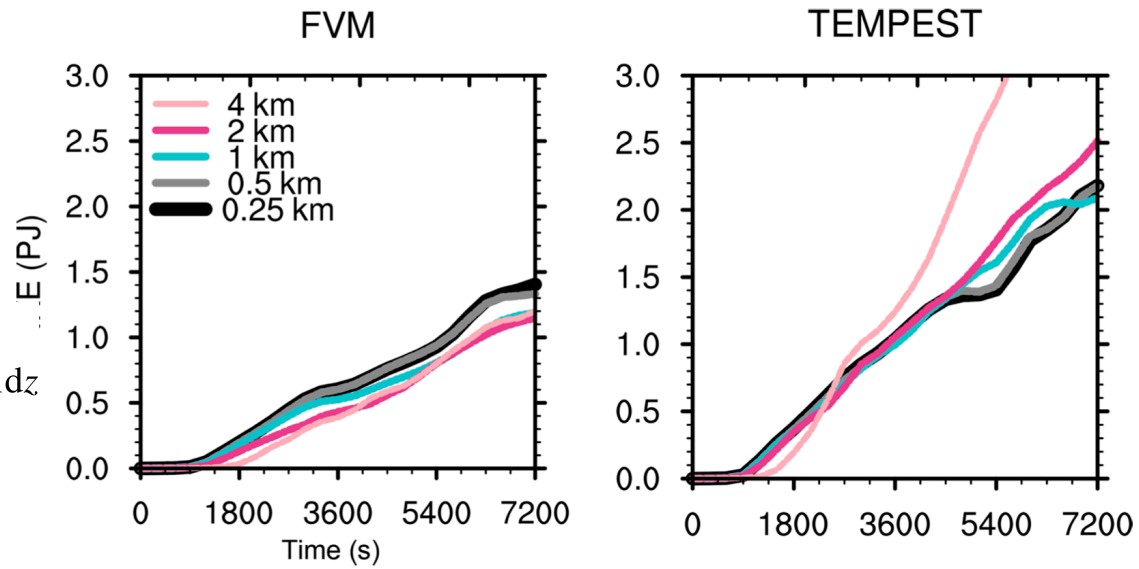
$$\mathrm{IKE}(t) = \frac{1}{2}\int_0^{z_t}\int_0^{A_e} \rho\left(u'^2 + v'^2 + w'^2\right) \mathrm{d}A\mathrm{d}z$$